Croatian Society for Materials Protection

Metalurgija/Metallurgy

Vol. 65 No. 4 / 2026

Corrosion resistance of W600 hot work tool steel in artificial rainwater and 3.5 % NaCl solution

Sandra Brajčinović [1], Anita Begić Hadžipašić [1,*], Jožef Medved[2] and Franjo Kozina[1]

https://doi.org/10.64486/m.65.4.13

[1] Faculty of Metallurgy, University of Zagreb, Aleja Narodnih Heroja 3, 44000 Sisak, Croatia; smitic@simet.unizg.hr, begic@simet.unizg.hr, fkozin@simet.unizg.hr
[2] Faculty of Natural Sciences and Engineering, University of Ljubljana, Aškerčeva Cesta 12, 1000 Ljubljana, Slovenia; jozef.medved@ntf.uni-lj.si
* Correspondence: begic@simet.unizg.hr

Type of the Paper: Article
Received: March 13, 2026
Accepted: April 29, 2026

Abstract: This paper studied the corrosion resistance of W600 tool steel in artificial rainwater and 3.5 % NaCl solution. The equilibrium phase diagram was determined from the material's chemical composition, with calculations and thermodynamic simulations carried out using Thermo-Calc software, enabling accurate prediction of stable phases as a function of temperature and composition. According to the obtained projections, the solidification and precipitation of individual phases at characteristic temperatures was read. Following the completion of the electrochemical measurements, insight into the corrosion behavior of the tested sample was provided. Electrochemical tests showed a decrease in charge transfer resistance and an increased corrosion rate in the 3.5 % NaCl solution, indicating inadequate resistance in a chloride-containing solution, attributed to the formation of a thin oxide layer caused by the attack of chloride ions from the solution. Metallographic analysis confirmed the occurrence of slowly progressing pitting corrosion in chloride solution, while no significant changes were observed after testing in artificial rainwater. The lower rate of pitting corrosion was attributed to the martensitic microstructure with fine needle-like morphology with uniformly distributed carbides in the W600 tool steel. Such investigations are essential for understanding material behavior in aggressive environments and for reliably predicting its durability in real applications.

Keywords: hot work tool steel; corrosion resistance; corrosion parameters; impedance; microstructure

1. Introduction

Tool steels are most frequently used in tool, spring, engine part and permanent mold production. In order to obtain good functional properties such as hardness, wear resistance, toughness, dynamic durability, resistance to oxidation and corrosion, tool steels are heat treated [1,2].

The selection of adequate metallic material is very often based on its corrosion behavior under the work environment conditions. The corrosion process initiates at the surface and progresses deeper into the metallic material at certain rates. Consequently, chemical composition and properties of the metallic material change at the local level. Corrosion process can comprehend partial or complete dissolution of the material [3,4].

Favorable functional properties of tool steel are achieved through the addition of one or more alloying elements. There are two basic alloying systems that increase corrosion resistance of tool steel by improving the efficacy of the protective surface layer. The first alloying system concerns reduction of non-metallic inclusion content in oxide layer, while the other leads to more significant changes in oxide layer characteristics. Furthermore, the corrosion behavior of tool steel can be influenced by the microstructure constituent's development resulting from chemical composition and heat treatment. Adequately applied heat treatment may enhance the corrosion resistance of tool steel [5,6].

Polluted urban atmospheres can have a negative effect on surface conditions and properties of metallic materials. During storage, delivery and utilization, tool steels are often exposed to harmful atmospheric conditions such as rain or chloride containing solutions. Under such conditions, an accelerated corrosion process may occur [7,8].

Most tool steels are subjected to the development of pitting corrosion during contact with solution containing aggressive ions. Pitting corrosion is a local form of corrosion that affects certain parts of the metal surface. It occurs when the continuity of the protective surface layer is broken [9,10]. Typically, ion activity is initiated at the inclusion–matrix interface because of the ingress of an aggressive environment. Those areas of increased ion activity become anodic, while the rest of the protective surface layer behave as a cathode. An aggressive medium causes rapid dissolution of the anodic areas [11–13]. Since only small damage can be observed on the tool's surface, pitting corrosion represents major obstacle during industrial application of tool steel. Understanding tool steel's tendency toward pitting corrosion is important in predicting the corrosion progression for the given working conditions. In order to fully comprehend the pitting corrosion mechanism, it is necessary to investigate the conditions under which the pitting initiates and progresses. The initial stage of pitting refers to the formation of the first small pit due to the breakdown of the protective film and anodic reactions on the metal surface. The progression of pitting comprehends dissolution of metal matrix or precipitates during reaction between ions and microstructure constituents [14,15]. The behavior of the metallic material exposed to the specific medium for a given time interval can be evaluated using electrochemical testing. Different electrochemical methods can be used to clarify corrosion mechanisms and characterize efficacy of protective films based on selected corrosion parameters [16,17].

Estimating corrosion behavior of tool steel in natural water is important due to the presence of free carbonic acid. In this type of environment carbonic acid has a harmful effect on protective surface layer and accelerates the corrosion reaction. The complete dissolution of surface layer occurs in sea water environments containing chloride ions. For this reason, most conventional electrochemical techniques are based on the addition of compounds that influence the formation of a protective surface layer with specific properties [16,17].

In addition to electrochemical testing, the metallographic analysis is used to characterize the behavior of different microstructural constituents in certain media, and linking the influence of chemical composition on surface stability. Full characterization of metallic material properties enables its appropriate application, as well as adequate protection against corrosion [18,19]. The results of corrosion testing can be used for modeling and confirmation of chemical composition. Corrosion parameters can be used to design an optimal combination of alloying elements aimed at improving the corrosion resistance of steel. In industrial applications where it is not possible to replace existing steel with a new one, the corrosion parameters enable selection of suitable agent for protection against corrosion. These agents are in form of inhibitors as an additional coating on steels. The corrosion parameters of tool steels are not widely available in the literature, especially when it comes to steels for special applications and medias they are not usually in contact with. In the existing literature, most studies on the corrosion behavior of tool steels in chloride-containing environments are focused on conventional cold work and hot work steels, highlighting their pronounced susceptibility to pitting corrosion due to the action of chloride ions. Previous findings indicate that chemical composition, alloying element content, and heat treatment significantly influence resistance to localized corrosion [20–22]. However, available data on W600 steel are limited, particularly under simulated atmospheric conditions and chloride solutions, which further emphasizes the importance of this research in terms of comparison and expanding current knowledge.

https://doi.org/10.64486/m.65.4.13

The goal of this research is to determine corrosion parameters for W600 hot work tool steel in normal and very aggressive media. This will enable characterization of its corrosion behavior and prediction of microstructure degradation mechanism. The tests were performed in the previously prepared solution of artificial rainwater and 3.5 % NaCl. Various electrochemical testing techniques allowed the determination of corrosion parameters, offering an understanding of the corrosion behavior of the investigated tool steel sample. In addition to corrosion assessment, calculations of the equilibrium solidification sequence were carried out using Thermo-Calc software, together with metallographic analysis. The utilization of those two methods enabled correlation of corrosion parameters with microstructure constituents at the surface layer of analyzed tool steel sample.

2. Materials and Methods

2.1. Materials

The chemical composition of the tested tool steel sample is given in Table 1.

Table 1. Chemical composition of tested W600 hot work tool steel (mas. %)

C	S	Si	Cr	Ni	V	W	Co	Al	Fe
0.32	0.001	0.12	0.11	2.1	0.01	1.9	0.01	0.009	
Cu	**Mn**	**Mo**	**P**	**Sn**	**Ti**	**Nb**	**B**	**N**	balance
0.01	0.23	3.2	0.005	0.005	0.01	0.01	0.001	0.008	

The W600 steel grade belongs to the group of tool steels designed for hot work applications. For the tool steel W600, a separate international standard is usually not specified. Although it is distinctive in terms of its composition and properties, it can be classified within the broader category of hot-work steels according to the AISI/SAE classification of the W group, which includes steels intended for high-temperature processing with increased hardness and wear resistance [23].

The tested steel belongs to the grade W of tool steels and is characterized by austenitization and water quenching. The most important alloying elements in this group of steels are nickel (Ni), tungsten (W) and molybdenum (Mo). Nickel in steel increases toughness and corrosion resistance without promoting carbide formation. The carbide formation is promoted through the addition of W and Mo. The presence of tungsten and molybdenum carbides enhance the wear resistance, high-temperature strength, and hardenability of steel. Tungsten promotes the formation of FeW_3C, W_6C and WC carbides, and molybdenum creates Mo_2C carbides [19].

2.2. Thermodynamic Calculations

Using the obtained chemical composition, the equilibrium solidification sequence and phase reactions in both liquid and solid states were calculated with Thermo-Calc 2022a software. The equilibrium phase diagram was calculated using the TCFE12: Steel/Fe-Alloys v12.0. Considering that the steel samples were heat treated, the equilibrium thermodynamic calculations were used primarily to determine the type of carbide particles.

2.3. Sample Preparation

The standard metallographic preparation of grinding and polishing was used to achieve the appropriate surface quality of W600 tool steel sample. To limit the effect of the corrosive medium on exposed surface, the sample was mounted in electrically conductive mass using hot mounting device SimpliMet® 1000 [20]. Grinding and polishing were performed automatically using a PhenixBeta grinding/polishing machine equipped with a Vector LC Power Head. After sample preparation, rinsing was performed using distilled water and ethanol. To characterize the as-received microstructure of W600 tool steel, an extra specimen was prepared for etching with 2.0 % Nital solution, composed of 98 mL ethyl alcohol and 3 mL nitric acid.

https://doi.org/10.64486/m.65.4.13

2.4. Preparation of Solutions

Solutions of artificial rainwater and 3.5 % NaCl were used as test media for electrochemical measurements. A solution of 3.5 % NaCl was selected to simulate a seawater-type corrosive medium. The solution of artificial rainwater in continental parts was prepared with the addition of Na_2SO_4 and $NaNO_3$ to distilled water. Prior to and after testing, the solution pH was determined using a laboratory pH meter and conductivity meter. The initial pH of the 3.5 % NaCl solution was 6.82, and that of artificial rainwater was 6.46. It can be seen that these are slightly acidic solutions. After the electrochemical measurements, the pH of the solutions did not change significantly.

2.5. Electrochemical Tests (E_{corr}, EIS, Tafel)

The corrosion performance of the material was investigated through determination of the corrosion potential (E_{corr}), electrochemical impedance spectroscopy (EIS), and Tafel extrapolation analysis [20]. Experimental measurements were carried out at ambient temperature (19 ± 2) °C using a Parstat 2273 potentiostat/galvanostat, while the acquired data were continuously recorded in digital form. Electrochemical characterization was performed in a standard three-electrode glass cell arrangement, where the examined specimen acted as the working electrode, a saturated calomel electrode was used as the reference, and a platinum electrode served as the counter electrode. During measurement, all three electrodes were immersed in a working medium (artificial rainwater and 3.5 % NaCl solution; volume 200 mL).

The evolution of corrosion behavior was assessed by recording the corrosion potential (E_{corr}) over a duration of 1800 s during exposure to different media. Open circuit potential measurements were performed under open-circuit conditions, without external current flow between the working and counter electrodes.

Electrochemical impedance spectroscopy (EIS) measurements were carried out over a frequency range from 100 kHz to 10 mHz, using a sinusoidal perturbation amplitude of 5 mV. The impedance response was evaluated by fitting the experimental data in ZSimpWin 3.60 software, employing the equivalent electrical circuit model R(Q(R(QR))).

Potentiodynamic polarization tests were conducted within a potential range of −250 to +250 mV vs. E_{corr} at a scan rate of 1 mV/s. The obtained electrochemical parameters, including corrosion potential (E_{corr}), corrosion current density (I_{corr}), corrosion rate (v_{corr}), and anodic and cathodic Tafel slopes (b_a and b_c), were determined using PowerCorr™ and PowerSuite 2.58 software [24,25].

To ensure statistical reproducibility, multiple measurements are typically performed. In this study, each series of electrochemical measurements was conducted in duplicate, as the obtained polarization and impedance curves exhibited excellent agreement. The low variability between repeated measurements indicates good reproducibility of the experimental system.

2.6. Metallographic Examinations

For metallographic examination, an inverted optical microscope Olympus DP27 equipped with a motorized stage was used, while image acquisition and analysis were performed using the Stream Motion automated image processing system. The microstructural analysis at higher magnifications was performed using scanning electron microscope Tescan Vega LSH. The microstructural investigation was performed on the samples before and after electrochemical corrosion testing. The samples before corrosion testing were analyzed in polished and etched condition. The analysis of the samples in polished condition was used to determine the presence of non-metallic inclusions, while the microstructural constituents were identified after etching in Nital. Following corrosion testing, microstructural examination focused on the analysis of the exposed surface.

3. Results and discussion

Figure 1 illustrates the equilibrium phase diagram for W600 hot work tool steel, derived from its chemical composition. The invariant reactions, together with their crystallographic properties, are summarized in Table 2.

https://doi.org/10.64486/m.65.4.13

According to equilibrium phase diagram, the liquidus temperature of W600 tool steel is 1490 °C, while the solidus temperature is 1190 °C. The solid-state reactions initiate with solidification of austenite (γ-phase). The solid-state reactions relate to the precipitation of carbide particles initiating with formation of M_6C carbides at 1066 °C. The following reactions result in precipitation of MC carbides at 771 °C and $M_{23}C_6$ carbides at 351 °C. The Ac_3 temperature was recorded at 786 °C, while the Ac_1 temperature was recorded at 699 °C.

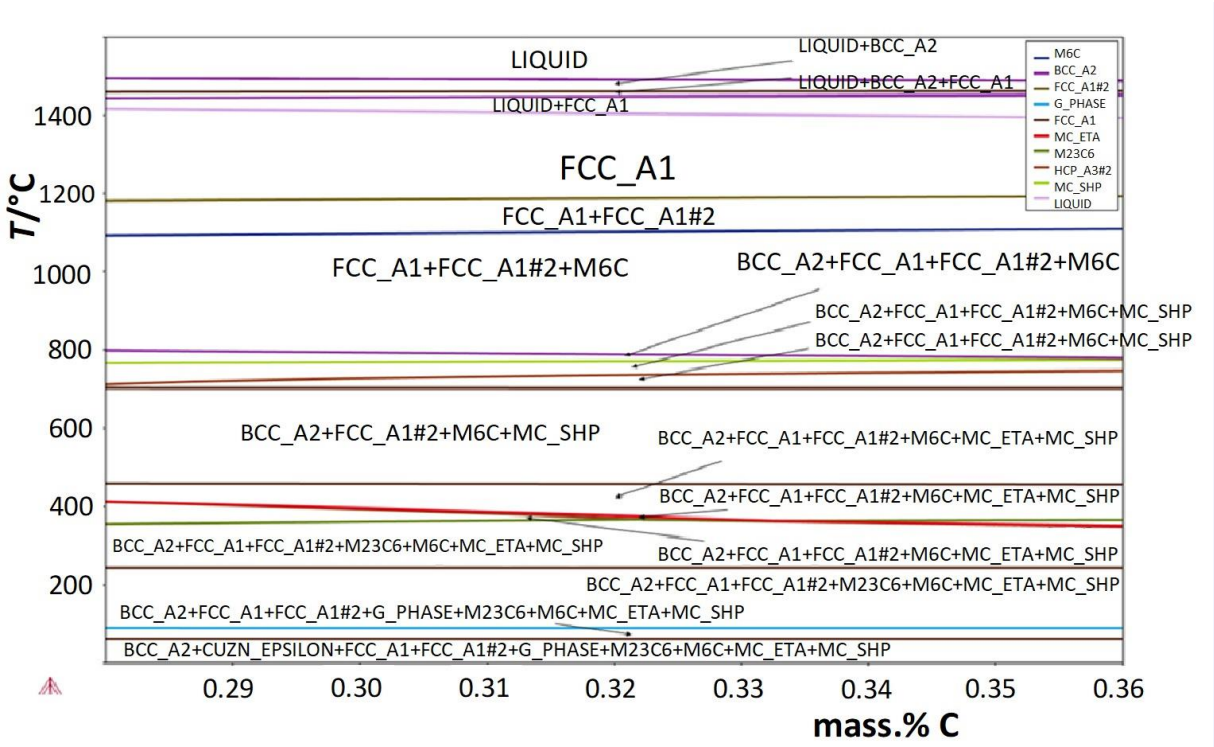

Figure 1. Calculated equilibrium phase diagram of W600 tool steel

Table 2. List of the stable phases from the calculation of the phase diagram using the Thermo-Calc method

List of Phases Using Thermo—Calc Method	Standard Phases
LIQUID+BCC_A2	L + δ
LIQUID+BCC_A2+FCC_A1	L + δ + γ
LIQUID+FCC_A1	L + γ
FCC_A1	γ
FCC_A1+M6C	γ + $(Mo, Fe, W)_6C$
BCC_A2+FCC_A1+M6C	α + γ + $(Mo, Fe, W)_6C$
BCC_A2+FCC_A1+M6C+MC_SHP	α + γ + $(Mo, Fe, W)_6C$ + (W, Mo)C
BCC_A2+M6C+MC_SHP	α + $(Mo, Fe, W)_6C$ + (W, Mo)C
BCC_A2+M23C6+M6C+MC_SHP	α + $(Cr, Fe, Mo)_{23}C_6$ + $(Mo, Fe, W)_6C$ + (W, Mo)C

Figure 2 presents how the open circuit potential of the tested tool steel varies over time in both media. In the sample that was exposed in the solution of artificial rainwater, the mean value of the open circuit potential of E_{ocp} = -140 mV was registered. For a sample exposed to the solution of 3.5 % NaCl, the mean value of the open circuit potential was E_{ocp} = -478.5 mV. Based on the obtained data, the open circuit potential in the 3.5 % NaCl solution is shifted toward more negative values, indicating greater instability of the sample in the chloride environment.

https://doi.org/10.64486/m.65.4.13

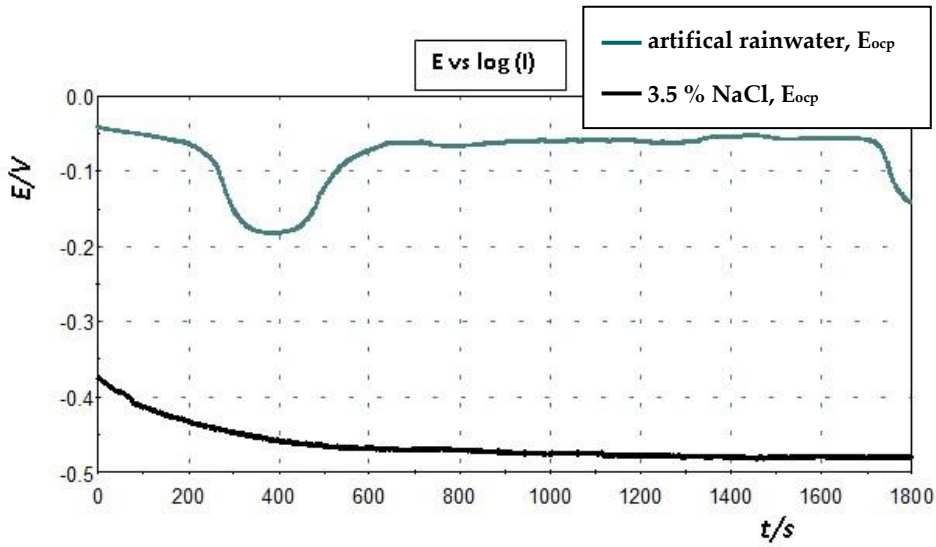

Figure 2. Variation of the open circuit potential over time for W600 tool steel in artificial rainwater and 3.5 % NaCl solution

The electrochemical impedance spectroscopy results are displayed using Nyquist and Bode plots (Figures 3 and 4). Impedance measurements were carried out over a frequency range from 100 kHz to 10 mHz, with a sinusoidal voltage amplitude of 5 mV.

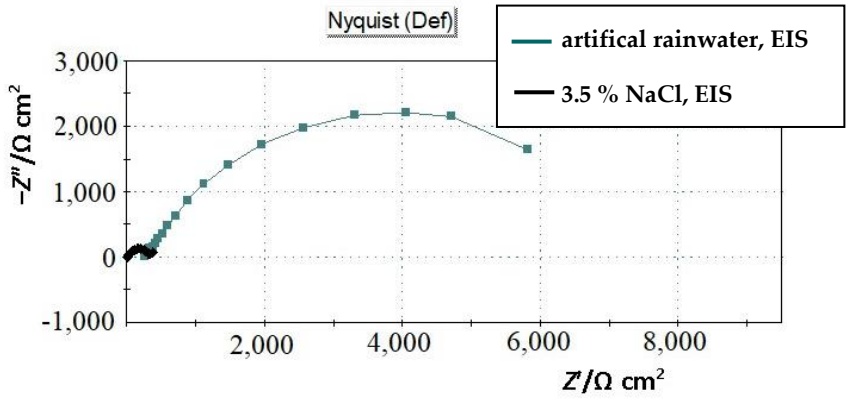

Figure 3. The comparative view of Nyquist's EIS diagrams obtained for W600 tool steel in artificial rainwater and a 3.5 % NaCl solution

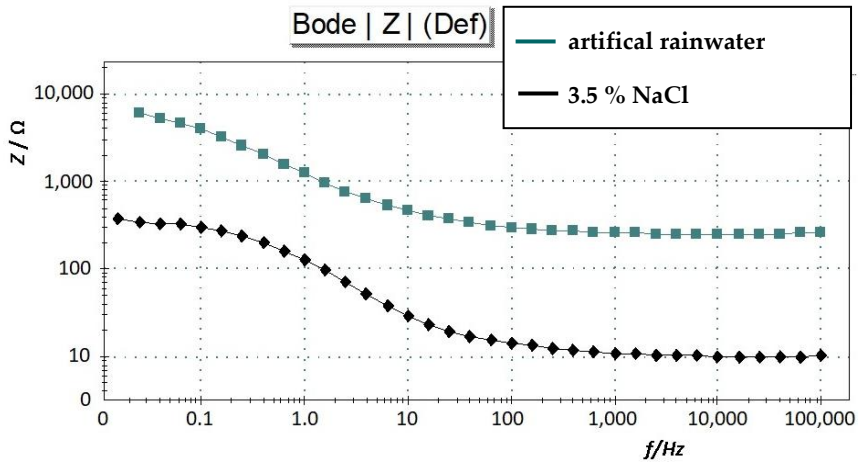

Figure 4. A comparative representation of the Bode EIS plots for W600 tool steel in artificial rainwater and a 3.5 % NaCl solution

https://doi.org/10.64486/m.65.4.13

The Nyquist EIS spectra obtained for the tested sample in both media (Figures 5 and 6) were fitted using ZSimpWin 3.60, applying an appropriate equivalent electrical circuit model, R(Q(R(QR))). The fitted results indicate good agreement between the simulated and experimental curves, with a deviation on the order of 10^{-4}. The measurement error was below 5 %, which is generally considered acceptable for this type of analysis [26].

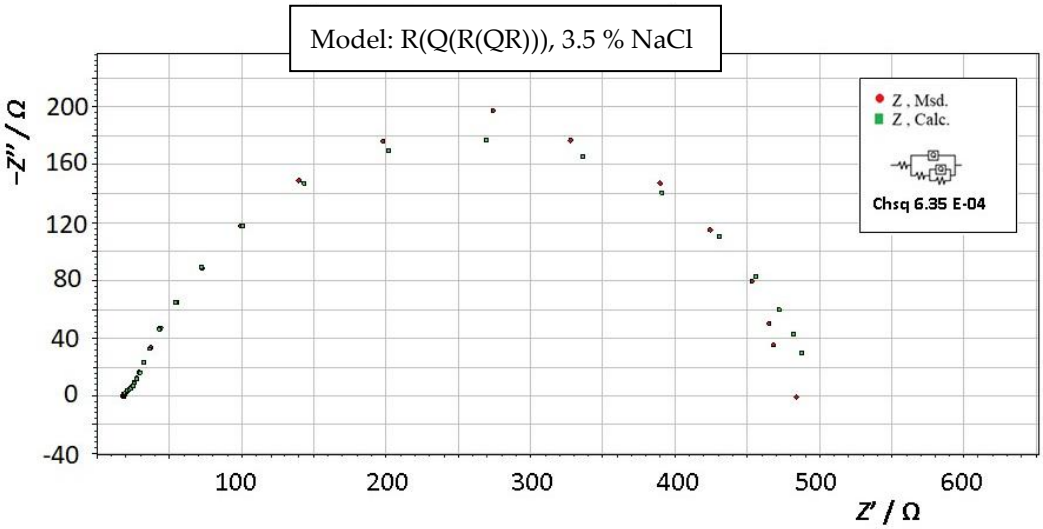

Figure 5. Modeling of the obtained Nyquist EIS spectrum for sample in 3.5 % NaCl solution

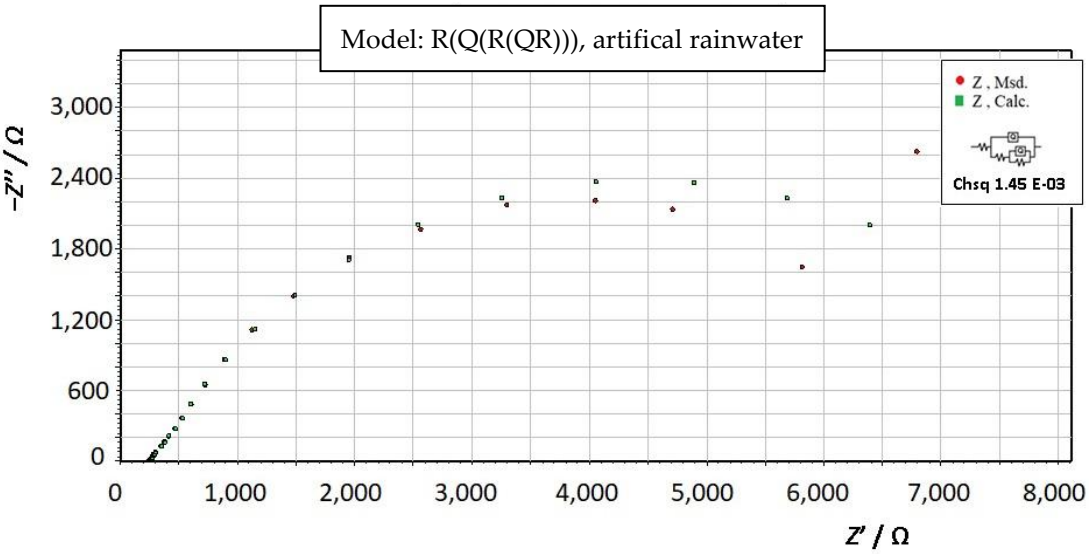

Figure 6. Modeling of the obtained Nyquist EIS spectrum for sample in artificial rainwater

The R(Q(R(QR))) equivalent circuit was selected based on its widespread use in the literature and its proven suitability for modeling electrochemical behavior of steel systems, particularly in corrosion-related EIS studies [27–29]. This model enables a detailed interpretation of complex electrochemical phenomena occurring on the surface of hot work steels, which cannot be achieved using a simple R–C model. The selected model is used because it provides a good description of the electrochemical behavior of systems involving a heterogeneous surface and the formation of a protective oxide layer. Each element of the equivalent circuit has its own physical meaning. The resistance R represents the electrolyte resistance, i.e., the resistance of the solution between the working and reference electrodes. The element Q (constant phase element, CPE) is used instead of an ideal capacitor to describe non-ideal capacitive behavior arising from surface roughness, heterogeneity, and the distribution of reaction sites. The R(QR) part of the model refers to processes occurring at the phase

https://doi.org/10.64486/m.65.4.13

boundary—the inner R represents the charge transfer resistance, while the corresponding Q describes the capacitance of the double layer of the oxide film.

Bode's diagram is another way of showing the impedance spectra. In that instance polarization resistance dominates at lower frequencies (f), while electrolyte resistance dominates higher frequencies. The phase angle achieves its highest value at medium frequencies. The presentation of the Bode diagram indicates that the metal/surface film/electrolyte system modelling also takes into account the transfer of the substance through the surface layer [26,30]. The presented spectra after measurement show that there is a decrease in the impedance of the system in a more aggressive medium due to the presence of chloride ions.

The Nyquist impedance plots of the sample measured in artificial rainwater and 3.5 % NaCl solution exhibit a depressed semicircular shape, which is characteristic of solid electrode systems. This behavior indicates non-ideal capacitive response, typically associated with surface heterogeneities and roughness. The diameter of the semicircle reflects the charge transfer resistance, suggesting differences in corrosion resistance between the two media. Figure 3 shows that the width of the Nyquist semicircle decreases in 3.5 % NaCl solution. This means that lower charge transfer resistance R_{ct} is expected in this solution, and therefore less corrosion resistance compared to the solution of artificial rainwater.

These facts are confirmed by the impedance parameters obtained after the modeling of Nyquist's EIS spectrum. The impedance parameters obtained for the tested W600 tool steel are summarized in Table 3, together with the arithmetic mean and standard deviation of the charge transfer resistance.

Table 3. Fitted EIS parameters of the tested W600 tool steel

Medium	No.	E_{corr} vs. SCE	R_{el}	$Q_{dl} \times 10^6$	n	R_{ox}	$Q_{dl} \times 10^6$	n	R_{ct}	$\bar{R}_{ct} \pm SD$
		mV	Ωcm²	Ω⁻¹sⁿcm⁻²		Ωcm²	Ω⁻¹sⁿcm⁻²		Ω cm²	Ω cm²
Artificial rainwater	1.	−141.0	252.5	238.3	0.6	1767.0	27.0	1.0	6747.0	6749.0 ± 2.8
	2.	−139.0	250.0	237.9	0.6	1760.0	27.1	1.0	6751.0	
3.5 % NaCl	1.	−480.0	10.0	1336.0	0.7	12.96	444.5	0.9	353.6	382.1 ± 40.3
	2.	−477.0	9.8	1329.0	0.7	12.00	372.5	0.9	410.6	

SD – standard deviation

After the artificial rainwater test, the W600 tool steel sample showed higher oxide (R_{ox}) and charge transfer (R_{ct}) resistances, indicating the development of a thicker protective surface layer upon exposure to the artificial rainwater. Contrarily, in the solution of 3.5 % NaCl lower values for R_{ox} and R_{ct} were registered. This means that the created protective layer is thin enabling aggressive ions to penetrate the metal more easily leading to the increase in corrosion rate.

The results obtained from electrochemical impedance spectroscopy are consistent with the corrosion parameters derived from the Tafel extrapolation method. Potentiodynamic polarization measurements were carried out in the potential range from −250 mV to +250 mV vs. E_{corr}. The corrosion parameters are presented in Table 4, together with the arithmetic mean and standard deviation of the corrosion rate, while the polarization curves of the tested sample in both solutions are shown in Figure 7.

Table 4. Electrochemical corrosion parameters of the tested W600 tool steel

Medium	No.	E_{corr} vs. SCE	b_a	b_c	I_{corr}	v_{corr}	$\bar{v}_{corr} \pm SD$
		mV	mV dec⁻¹	mV dec⁻¹	Acm⁻²	mm yr⁻¹	mm yr⁻¹
Artificial rainwater	1.	−124.14	214.89	167.90	1.58×10⁻⁶	0.07	0.07 ± 0.00
	2.	−126.45	217.76	166.27	1.58×10⁻⁶	0.07	
3.5 % NaCl	1.	−454.51	132.55	632.66	125.89×10⁻⁶	2.54	2.53 ± 0.01
	2.	−455.55	129.00	629.18	125.89×10⁻⁶	2.52	

https://doi.org/10.64486/m.65.4.13

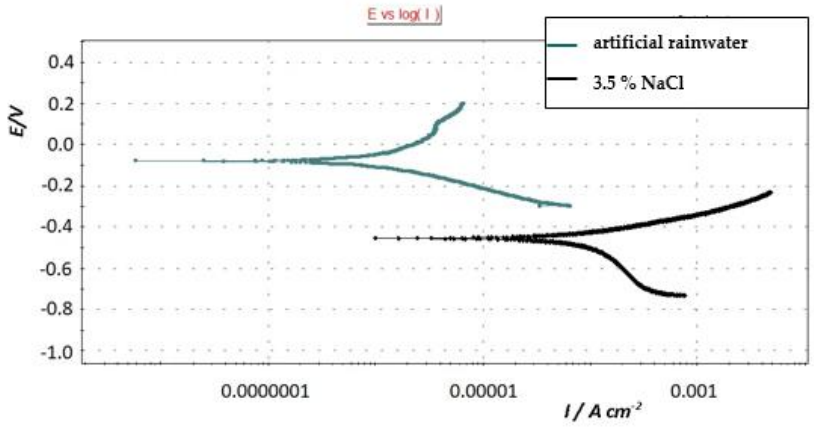

Figure 7. Potentiodynamic polarization curves of the tested W600 tool steel in artificial rainwater and 3.5 % NaCl solution

From the data in Table 4, it is evident that the much higher corrosion current density and corrosion rate of the tested sample v_{corr} was registered in a chloride medium. This indicates that W600 tool steel should not be used in medium that is similar to seawater. It is important to note that both potentiodynamic polarization and EIS tests were conducted after a 30-minute open-circuit potential stabilization period. Figure 8 displays the metallographic micrographs of the W600 tool steel prior to and following Nital etching. The microstructure of the sample in polished condition indicates the presence of non-metallic inclusions. Figure 8a reveals non-metallic inclusions that may adversely affect the corrosion resistance of the steel and represent potential sites for the initial phase of pitting. Since, the sample was not plastically deformed, it is not possible to determine the type of inclusions. Based on the chemical composition it can be assumed that present non-metallic inclusions are of aluminate and oxide type. The metallographic analysis identified a martensitic structure obtained through water quenching (Figure 8b).

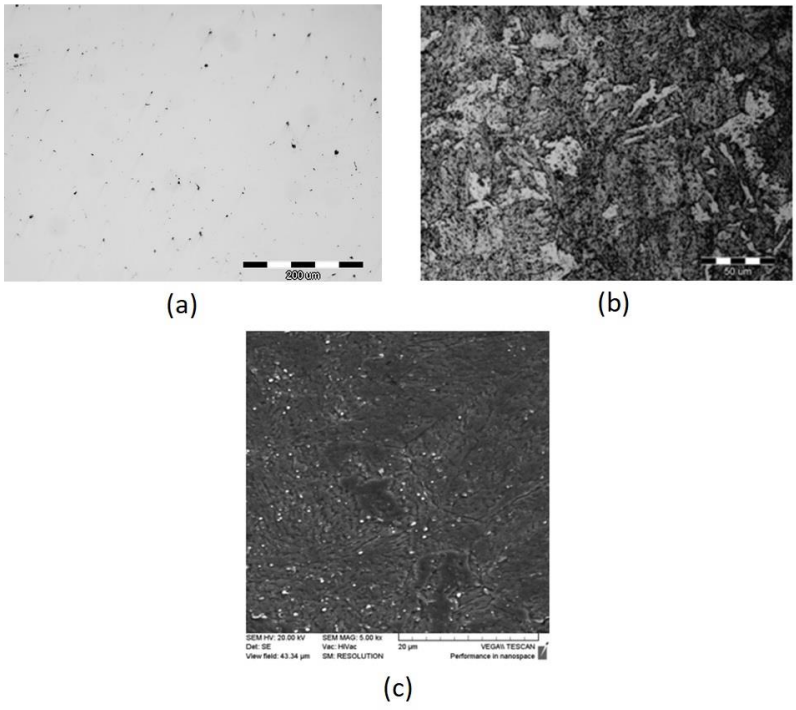

Figure 8. Microstructure of W600 tool steel: (a) before etching in polished condition, magnification 200x (light microscopy); (b) after etching in nital, magnification 500x (light microscopy); (c) after etching in nital, magnification 5000x (scanning electron microscope)

https://doi.org/10.64486/m.65.4.13

Metallographic analysis shows the needle form of martensite with the presence of secondary carbides. According to the literature [31–33], increase in tempering temperature enables growth and spheroidization of carbide particles. The uniformly distributed carbide particles are visible in scanning electron image at high magnification (Figure 8c).

The metallographic images after electrochemical testing are shown in Figure 9. Exposure to artificial rainwater did not result in any significant changes on the surface (Figure 9a and 9b). In contrast, the electrochemical testing in 3.5 % NaCl solution resulted in development of corrosion products (Figure 9c and 9d). Distribution of corrosion products is characteristic for pitting corrosion occurrence.

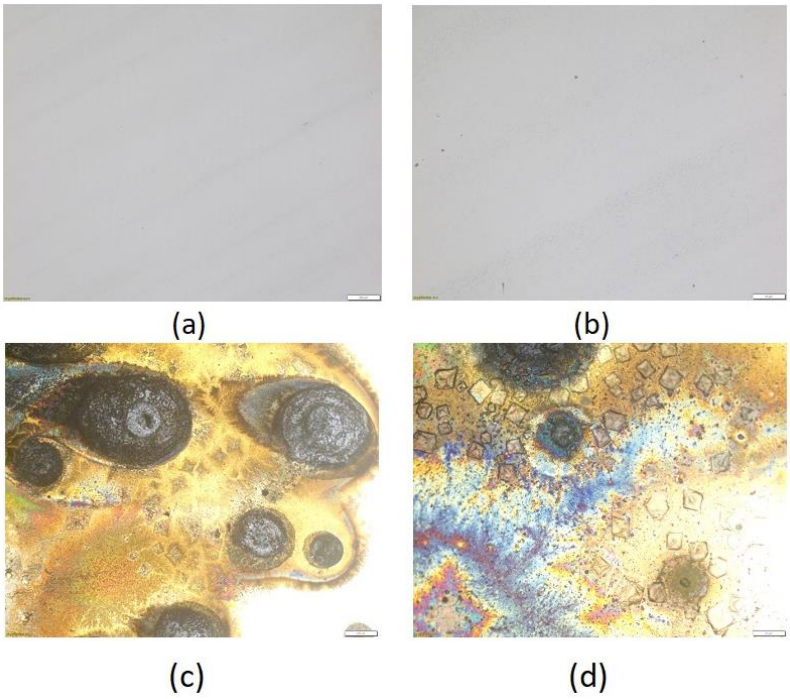

Figure 9. Microstructure of W600 tool steel in artificial rainwater and 3.5 % NaCl solution: (a) artificial rainwater: magnification 50x; (b) artificial rainwater: magnification 200x; (c) 3.5 % NaCl: magnification 50x; (d) 3.5 % NaCl: magnification 200x

It can be concluded that corrosion products and pitting corrosion resulted from chloride action. The repeated grinding and polishing indicated that corrosion occurred locally on the surface of the sample. The performed investigations indicate that the occurrence of pitting corrosion can cause major problems in industrial plants. Namely, chloride can accumulate in formed pits and encourage deeper penetration into the metallic material. In this study, carbides of the M_6C, MC, and $M_{23}C_6$ types were identified using Thermo-Calc simulations, and their precipitation was correlated with corrosion parameters and metallographic analyses. The presence of secondary carbides and their distribution influence the formation of a protective oxide layer and the local corrosion resistance of the material, as reflected in lower R_{ct} values and the occurrence of pitting corrosion in an aggressive chloride medium.

Furthermore, phase equilibria and temperature dependencies obtained from Thermo-Calc diagrams enable a better understanding of the conditions under which specific carbides form, helping to explain differences in material behavior in artificial rainwater and in a 3.5 % NaCl solution. Based on these results, a deeper interpretation of corrosion mechanisms is possible: an aggressive chloride medium disrupts the protective oxide layer, whereas in less aggressive conditions (artificial rainwater), the presence of carbides contributes to its formation and stability.

https://doi.org/10.64486/m.65.4.13

Considering that chromium is regarded as a beneficial alloying element, it is assumed that the presence of chromium carbides contributes to improved corrosion parameters after testing in artificial rainwater. The obtained corrosion parameters are consistent with the visual surface analysis, thereby establishing a clear relationship between microstructure and corrosion processes, further confirming the scientific contribution of this research.

Since no studies of this type have previously been reported for W600 tool steel, it is particularly important to investigate carbide precipitation that may contribute to improved corrosion properties. This is especially relevant in the design and development of new tool steels, where the selection and content of alloying elements can be tailored to promote the formation of desirable carbide phases.

Therefore, the main scientific contribution of this study lies in a comprehensive analysis of the corrosion resistance of W600 tool steel in two different media – artificial rainwater and 3.5 % NaCl – with a correlation of electrochemical results to phase equilibria and the microstructure of the material. The novelty of the research includes several aspects:

1. Application of thermodynamic modeling (Thermo-Calc) to predict the precipitation of carbides (M6C, MC, and M23C6) at specific temperatures, enabling a better interpretation of the material's behavior during experimental testing.
2. Combination of corrosive media – aggressive chloride solutions and simulated atmospheric conditions – allowing the assessment of material resistance under conditions relevant for industrial applications.
3. Correlation of electrochemical and metallographic analyses – changes in open-circuit potential, charge transfer resistance, occurrence of pitting corrosion, and microstructural characteristics – providing a detailed insight into corrosion processes and the resistance of W600 under different conditions.

Based on the obtained results, the engineering applications of the material can be clearly defined: W600 is suitable for moderately aggressive media and environments without high chloride concentrations, while its use in highly chlorinated conditions or during prolonged exposure is not recommended. Thus, the study contributes to a practical understanding of the corrosion behavior of this specific tool steel and provides guidance for its safe industrial application.

4. Conclusions

Electrochemical tests indicate significantly lower resistance of the material in an aggressive chloride medium (3.5 % NaCl) compared to artificial rainwater, as evidenced by a more negative open-circuit potential, lower charge transfer resistance, and higher corrosion rate.

Surface analysis further confirms the onset of pitting corrosion in the NaCl solution, while no changes were observed in artificial rainwater. The fine-grained martensitic microstructure of the tool steel with uniformly distributed carbide particles of types M6C, MC, and M23C6 was partly responsible for the slower process of pitting corrosion.

In conclusion, the W600 tool steel is suitable for use in moderately aggressive media and environments without high chloride concentrations. However, its application in highly chlorinated conditions or during prolonged exposure may lead to corrosion damage, and therefore its use under such conditions is not recommended.

https://doi.org/10.64486/m.65.4.13

Acknowledgments: The investigation was carried out as part of the Institutional Research Project the "Design and characterisation of innovative engineering alloys/products (KIIL)"financed by the EU – Next Generation EU. The views and opinions expressed are those of the author and do not necessarily reflect the official positions of the European Union or the European Commission. Neither the European Union nor the European Commission can be held responsible for them. The investigation was performed on equipment within the infrastructural scientific projects: Center for Founding - SIMET (Code: KK.01.1.1.02.0020); and the VIRTULAB - Integrated Laboratory for Primary and Secondary Raw Materials (Code: KK.01.1.1.02.0022).

References

[1] W. E. Bryson, *Heat treatment, selection and application of tool steels,* 2nd ed. Cincinnati, USA: Hanser Publications, 2013.

[2] G. Roberts, G. Krauss, R. Kennedy, *Tool Steels,* 5th ed. Materials Park, Ohio, USA: ASM International, 1998, https://doi.org/10.31399/asm.tb.ts5.9781627083584.

[3] R. W. Revie, H. H. Uhlig, *Corrosion and Corrosion Control: An Introduction to Corrosion Science and Engineering,* 4th ed. New Jersey, USA: A John Wiley & Sons, INC., Publication, 2008, https://doi.org/10.1002/9780470277270.

[4] E. D. D. During, *Corrosion Atlas, A Collection of Illustrated Case Histories,* 3rd ed. Amsterdam, The Netherlands: Elsevier Ltd., 2018.

[5] F. M. F. Al-Quran and H. I. Al-Itawi, "Effects of the heat treatment on corrosion resistance and microhardness of alloy steel," *European Journal of Scientific Research,* vol. 39, no. 2, pp. 251–256, 2010.

[6] N. B. Popov, *Corrosion Engineering Principles and Solved Problems.* Amsterdam, The Netherlands: Elsevier Ltd., 2015.

[7] S. Syed, "Atmospheric corrosion of materials," *Emirates Journal for Engineering Research*, vol. 11, no. 1, pp. 1–24, 2006.

[8] Stainless Steels in Architecture, Building and Construction. [Online]. Available: https://nickelinstitute.org/media/1613/11024-guidelines-for-corrosion-prevention.pdf [Accessed: Oct. 25, 2021].

[9] M. Schütze, M. Roche, R. Bender, *Corrosion Resistance of Steels, Nickel Alloys and Zinc in Aqueous Media.* Germany: Dechema, 2016.

[10] A. Abbas, A. Y. Adesina and R. K. Suleiman, "Influence of organic acids and related organic compounds on corrosion behavior of stainless steel–A critical review," *Metals,* vol. 13, Article no. 1479, 2023, https://doi.org/10.3390/met13081479.

[11] R. T. Loto, "Pitting corrosion evaluation and inhibition of stainless steels: A review," *Journal of Materials and Environmental Sciences,* vol. 6, no. 10, pp. 2750-2762, 2015. [Online]. Available: https://www.jmaterenvironsci.com/Document/vol6/vol6_N10/326-JMES-1736-2015-Loto.pdf [Accessed: Oct. 25, 2021].

[12] J. Nagler, "Pitting corrosion investigation of cantilever beams using F.E. method," *World Journal of Mechanics*, vol. 3, no. 2, pp. 89–100, 2013, https://doi.org/10.4236/wjm.2013.32007.

[13] Y. Kang, X. Leng, L. Zhao, B. Bai, X. Wang, and H. Chen, "Review on the corrosion behaviour of nickel-based alloys in supercritical carbon dioxide under high temperature and pressure," *Crystals,* vol. 13, no. 5, Article no. 725, 2023, https://doi.org/10.3390/cryst13050725.

[14] N. Perez, *Electrochemistry and corrosion science*. Boston, USA: Kluwer Academic Publishers, 2004.

[15] G. T. Burstein, C. Liu, R. M. Souto, and S. P. Vines, "Origins of pitting corrosion," *Corrosion Engineering, Science and Technology*, vol. 3, pp. 89–100, 2004, https://doi.org/10.1179/147842204225016859.

[16] S. Chen, L. Sun, and W. Li, "Effect of chloride threshold on pitting behavior of 316LN stainless steel in sour water solution by electrochemical analysis," *Materials and Corrosion*, vol. 74, pp. 242–252, 2023, https://doi.org/10.1002/maco.202213414.

[17] M. Muhammed, M. Javidani, M. Heidari, and M. Jahazi, "Enhancing the tribological performance of tool steels for wood-processing applications: A comprehensive review," *Metals*, vol. 13, Article no. 1460, 2023, https://doi.org/10.3390/met13081460.

[18] L. Lai, P. Chekhonin, S. Akhmadaliev, J.-E. Brandenburg, and F. Bergner, "Microstructural characterization of reactor pressure vessel steels," *Metals*, vol. 13, Article no. 1339, 2023, https://doi.org/10.3390/met13081339.

[19] R. Sunulahpašić, M. Oruč, *Tool Steels and Other Tool Materials* (in Bosnian). Zenica, Bosnia and Herzegovina: University of Zenica, Faculty of Metallurgy and Technology, 2019.

[20] D. L. Buruiană, A. C. Mure, N. Bogatu, V. Ghisman, E. E. Herbei, V. Başliu, "Corrosion Tendency of S235 Steel in 3.5 % NaCl Solution and Drinking Water During Six Months of Exposure," *Materials,* vol. 17. no. 23, pp. 5979, 2024, https://doi.org/10.3390/ma17235979

[21] W. Beom, K. Yun, C. J. Park, H. Ryu, Y. Kim, "Comparison of influences of NaCl and $CaCl_2$ on the corrosion of 11 % and 17 % Cr ferritic stainless steels during cyclic corrosion test," *Corrosion Science,* vol. 52, no. 3, pp. 734-739, 2010, https://doi.org/10.1016/j.corsci.2009.10.033

[22] S. Hastuty, A. Nishikata, T. Tsuru, "Pitting corrosion of Type 430 stainless steel under chloride solution droplet", *Corrosion Science,* vol. 52, no. 6, pp. 2035-2043, 2010, https://doi.org/10.1016/j.corsci.2010.02.031

[23] Steel grades, "W6 tool steel," Steel Grades, n.d. [Online]. Available: https://www.steel-grades.com/Steel-Grades/tool-die-steels/70/7249/W6.html?utm_source=chatgpt.com#google_vignette [Accessed: March 30, 2026].

[24] S. Brajčinović, A. Begić Hadžipašić, and J. Medved, "Inhibitory effect of commercial inhibitor VCI 379/611 on the corrosion behaviour of HTCS-130 tool steel for hot work," *Metals*, vol. 12, Article no. 966, 2022, https://doi.org/10.3390/met12060966.

[25] S. Brajčinović, A. Begić Hadžipašić, J. Medved, and S. Kožuh, "Corrosion resistance of cementing steel X19NiCrMo4 in medium of 5 % NaOH and 5 % H_2SO_4," in *Proceedings Book of 19th International Foundrymen Conference: Humans – Valuable Resource for Foundry Industry Development*, Split, Croatia, pp. 249-259. [Online]. Available: https://repozitorij.simet.unizg.hr/en/object/simet:637/FILE0 [Accessed: Nov. 16, 2021].

[26] A. Lasia, *Electrochemical Impedance Spectroscopy and its Applications*. New York, USA: Springer, 2014, https://doi.org/10.1007/978-1-4614-8933-7.

[27] R. Zhang, D. Sur, K. Li, J. Witt, R. Black, A. Whittingham, J. R. Scully, J. Hattrick-Simpers, "Bayesian assessment of commonly used equivalent circuit models for corrosion analysis in electrochemical impedance spectroscopy," *npj Materials Degradation,* vol. 8, Article no. 120, 2024. https://doi.org/10.1038/s41529-024-00537-8.

[28] H. Gerengi, M. Cabrini, M. M. Solomon, E. Kaya, "Understanding the corrosion behavior of the AZ91D alloy in simulated body fluid through the use of dynamic EIS," *ACS Omega,* vol 7, no. 14, pp. 11929−11938, 2022. https://pubs.acs.org/doi/10.1021/acsomega.2c00066.

[29] B. Sarac, E. Sharifikolouei, Y, Zheng, E. Yüce, A. Asci, J. Keckes, A. S. Sarac, J. Eckert, "Electrochemical impedance behavior and corrosion resistance of amorphous 316-type stainless steel microfibers in saline environment," *Materials Today Communications,* vol. 44, p. 112178, 2025. https://doi.org/10.1016/j.mtcomm.2025.112178.

[30] I. Bačić, "Enhancement of Corrosion Protection of Stainless Steel by Nanostructured Sol–Gel ZrO_2 Films," Ph.D. dissertation, Faculty of Science, University of Zagreb, Zagreb, Croatia, 2016. [Online]. Available: https://urn.nsk.hr/urn:nbn:hr:217:213329.

[31] H. Schumann, *Metallographie (in Serbian).* Beograd, Serbia: Faculty of Technology and Metallurgy, 1981.

[32] L. F. Mondolfo, O. Zmeskal, *Engineering Metallurgy (in Croatian)*. Zagreb, Croatia: Technical Book, 1967.

[33] M. Durand-Charre, *Microstructure of Steels and Cast Irons.* Berlin/Heidelberg, Germany: Springer, 2003, https://doi.org/10.1007/978-3-662-08729-9.

https://doi.org/10.64486/m.65.4.13